Transactions of the Materials Research Society of Japan 29[5] 2229-2232 (2004)

The Intercalation of Some Metal Ammine Complexes into Ti layered Oxides by Electrostatic Self-assemble Deposition (ESD) Technique

Ugur Unal, Yasumichi Matsumoto and Michio Koinuma
Department of Applied Chemistry, Faculty of Engineering, Kumamoto University,
Kurokami 2-39-1, Kumamoto 860-8555 Japan
Fax: 81-96-342-3659 e-mail: yasumi@gpo.kumamoto-u.ac.jp

A new method for the intercalation into Ti layered oxides was discussed in this study. Intercalation was performed by mixing exfoliated $H_xTi_{(2-x/4)}\square_{x/4}O_4$ colloidal solution with a metal ammine complex in a pH 8.5 buffer solution to avoid any possible metal hydroxide formation. Negatively charged Ti-O nanosheets in the solution combined with the metal ammine cations due to the electrostatic principles. The resulting intercalated Ti-O oxide was deposited on a Pt electrode either by electrodeposition or spin coating method. SEM microphotographs showed that the deposition of submicron sheets took place parallel to the substrate surface. The layer distance of the intercalated samples were calculated to be around 11.5 Å for hexaammine complexes. Heat treatment of the films led into subsequent anatase and rutile phase formation with increasing temperature. Electrochemical behavior of the films was also analyzed. The results indicated that the intercalation of complex compounds into the layered materials is possible with this new technique.

Keywords: intercalation, layered oxides, electrophoretic deposition, photochemistry, and electrochemistry

1. INTRODUCTION

Compounds with a layered structure have interesting chemical properties that largely change with the intercalation[1,4], ion-exchange[5,6], and pillaring[7] into the interlayer. These types of layered materials have some applications in the fields of photocatalysis, photoluminescence and photoelectrochemistry. Some stable intercalated cations and molecules will act as an electron donor, an acceptor, or a recombination center due to their energy levels with respect to the host layers, and may bring about drastic changes in physical and/or chemical properties. It is very important for the development of new photocatalysts and electrodes in photocells to know the effects of the stable intercalated species on the electrochemical and photoelectrochemical properties. Moreover, some energy levels vs. solution can sometimes be derived from these properties, which are very useful when discussing the mechanism in the photocatalysis and other devices using an electron transfer. However, the electrochemical and photoelectrochemical behavior of the M_1-O layered oxides intercalated with stable cations such as transition metals and metal complexes has yet to be studied.

In this study, we demonstrate a new technique to prepare intercalated Ti-O layered oxides by ESD, the phase-change behavior of the intercalated films under heat-treatment and the electrochemical and photoelectrochemical properties of the intercalated Ti-O oxide films.

2. EXPERIMENTS

$Cs_xTi_{(2-x/4)}\square_{x/4}O_4$ (C-Ti oxide) as the starting material was prepared by the complex polymerization method[8]. The proton exchange and exfoliation processes were explained in detail elsewhere[1]. Ethylamine and tetrabutylammine aqueous solutions were used for the exfoliation of the proton exchanged Ti-O oxide. The intercalated Ti-O layered structures were prepared by mixing 0.01 M aqueous solution of the metal complex salt with 10 ml of the exfoliated colloidal solution at a pH of 7 or 8.5 to avoid any possible hydroxide formation. Apart from the other complex intercalated Ti-O oxides, the $Ag(NH_3)_2^+$ intercalated Ti-O oxides were prepared by dissolving its Cl^- salt in water by adding an excess amount of concentrated ammonium solution until the salt dissolved completely. When the $Ru(bpy)_3^{2+}$ intercalated Ti-O oxides were prepared, TBA exfoliated Ti-O nanosheet solution was used instead. The Ru/Ti ratio was 1 after the addition. When the negatively charged Ti-O nanosheets suspended in the solution come in contact with the $M(NH_3)_x^{y+}$ cations, they combine due to the electrostatic self-assemble deposition (ESD) mechanism to result in the precipitates. The precipitate consists of a single-phase Ti-O layered oxide intercalated with metal-complex cations. Following the rinsing of the precipitates with water and acetone subsequently, the intercalated Ti-O oxide was deposited on a Pt or ITO electrode by either

electrophoretic deposition (EPD) method or applying the precipitate onto the electrode directly. The films were examined by using Scanning Electron Microscope (SEM), X-ray Diffractometer (XRD), Induced Coupled Plasma (ICP), X-ray Photoelectron Spectrometer (XPS), Thermal analysis (TG/DTA), and Fourier Transformed Infrared Spectrometer (FTIR). All electrochemical experiments were carried out in a conventional three-electrode electrochemical cell in the presence of 0.1 M K_2SO_4 as an electrolyte. The counter and reference electrodes were Pt and a saturated Ag/AgCl electrode, respectively. A 500W ultra-high pressure Hg lamp was used as the ultraviolet (UV) light source to measure the photoelectrochemical properties. Cyclic voltammograms (CV) were measured under potential sweep rate of 20 mVs^{-1}. The electrolytes were saturated with N_2 prior to the electrochemical measurements.

3. RESULTS AND DISCUSSION

The addition of the exfoliated Ti-O nanosheet colloidal solution into the aqueous solution containing metal complexes resulted in the formation of the Ti-O layered oxides intercalated with the metal complex cations due to the electrostatic principles governing the deposition. The ESD resulting in the intercalation occurred immediately after the colloidal solution was added to the solution. The SEM micrographs of the deposited films exhibited a mosaic-like pattern of the film surface and revealed that the intercalated sheet formed from approximately piled 10 units with a uniform size of 1 μm on its planar surface. The orientation of the intercalated Ti-O sheets was parallel to the surface of the substrate. The XRD patterns of the Ti-O films intercalated with metal complexes showed a highly crystalline layered single phase oriented in (0k0) direction as seen in Figure 1.

The layer distances of the films are given in Table 1 together with the M/Ti atomic ratio and estimated compositions. The M/Ti atomic ratios were determined from the ICP and/or XPS analyses. One mol of the original $Cs_{0.76}Ti_{1.81}O_4$ powder requires 0.76 mol intercalated monovalent cations in the composition to compensate the negative charge of the Ti-O layer. The compensation of the positive charge deficiency was attained by intercalation of the H^+ and/or H_3O^+ ions, because no other ion such as Cl- or ethylamine with positive charge was observed according to the XPS. The presence of the complex molecules was also confirmed using XPS and FTIR analyses. Comparing the interlayer distances and the related molecular size of the complex, we can conclude that the complex molecules presents within the interlayer in a single layer arrangement. According to the TG/DTA data, water molecules were also intercalated together with the complexes and will be located in the cavities between the complex molecules and the Ti-O layers. Apart from the other intercalated Ti-O oxide, the orientation of the $Ag(NH_3)_2^+$ in the interlayer in an inclined or a horizontal form will bring about the direct interaction between the Ag^+ and the host Ti-O with a negative charge to some extent via the electrostatic force. The direct interaction will be suppressed by the surrounding NH_3 ligands in the hexaammine complex cations. This causes a difference in the electrochemical behavior as stated in a later section.

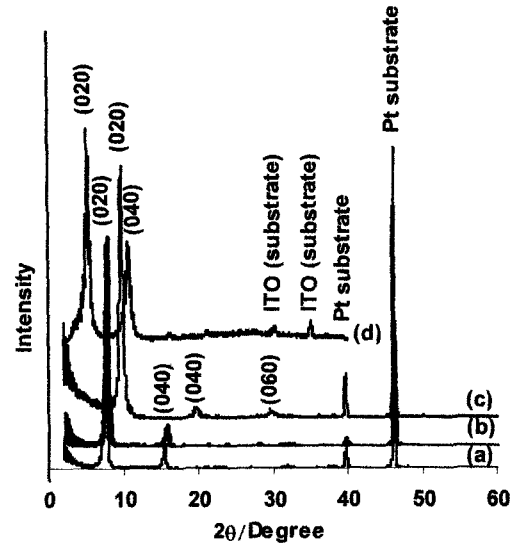

Figure 1. XRD patterns of some Ti-O layered oxides intercalated with metal complex cations; (a) $Ru(NH_3)_6^{3+}$-TiO, (b) $Co(NH_3)_6^{3+}$-TiO, (c) $Ag(NH_3)_2^+$-TiO, (d) $Ru(bpy)_3^{2+}$-TiO

The heat-treatment of the hexaammine intercalated samples brought about a decrease in the interlayer distance due to the structural change and the decomposition of the molecules by 225 °C, at which the weight loss of the ammine complexes start. The TG/DTA curves of the hexaammine intercalated Ti-O samples revealed four main weight loss regions and the weight loss regions between room temperature to about 150 °C and from 150 °C to about 250 °C were assigned to the removal of the free and intercalated water, respectively. Since the starting point of the weight loss

Table 1. Layer distances and atomic ratios of the complex intercalated Ti-O films. The compositions were calculated from the atomic ratio (ICP and XPS) and water content (TG/DTA).

Intercalated Metal Complex	Layer Distance (Å)	M/Ti Atomic Ratio	Composition
$Ru(NH_3)_6^{3+}$	11.47	0.22	$[Ru(NH_3)_6^{3+}]_{0.19}Ti_{1.81}O_4 \cdot 2.1H_2O$
$Co(NH_3)_6^{3+}$	11.41	0.12	$[Co(NH_3)_6^{3+}]_{0.22}Ti_{1.81}O_4 \cdot 2.4H_2O$
$Ag(NH_3)_2^+$	8.99	0.4	$[Ag(NH_3)_2^+]_{0.32}Ti_{1.81}O_4 \cdot 0.7H_2O$
$Ru(bpy)_3^{2+}$	16.6	0.04	$[Ru(bpy)_3^{2+}]_{0.07}Ti_{1.81}O_4 \cdot 2.5H_2O$

of the ammine complexes overlaps with the release of intercalated water in the second range, the amount of the intercalated water was calculated from the weight loss in the range of 150 to 225 °C. The values given in Table 1, therefore, have some errors due to neglecting the potential loss of the intercalated water over 225 °C. The heat treatment of the hexaammine complex intercalated Ti-O oxides resulted in the decrease and subsequent destruction of the layer distance. The heat-treatment over 400 °C brought about the formation of the anatase and rutile phases. $Ag(NH_3)_2^+$ intercalated Ti-O oxide, in which only small amount of water molecules existed kept its layered structure up to 400 °C without any abrupt change.

The $Ru(bpy)_3^{2+}$ intercalated sample lost weight in three steps. The starting point of the third step at 320 °C was attributed to the decomposition of the intercalated $Ru(bpy)_3^{2+}$ cations, since the decomposition of the complex itself starts at 320 °C by oxidation. The XRD pattern of the film revealed that the film maintained its layered structure without any change. The heat-treatment over the decomposition temperature of the $Ru(bpy)_3^{2+}$ complex brought about the destruction of the layered structure, as seen in Figure 2.

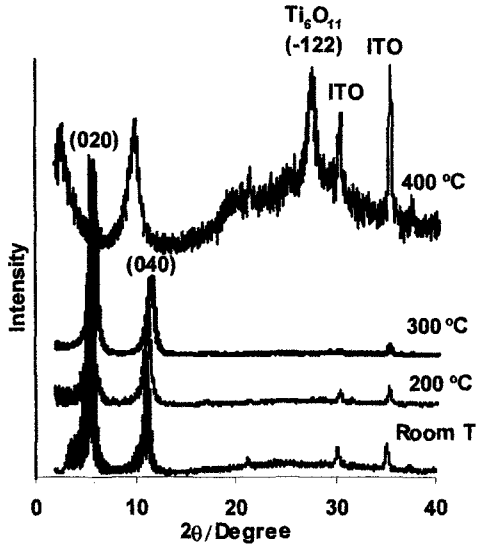

Figure 2. XRD pattern of the $Ru(bpy)_3^{2+}$ intercalated oxide heated at different temperatures.

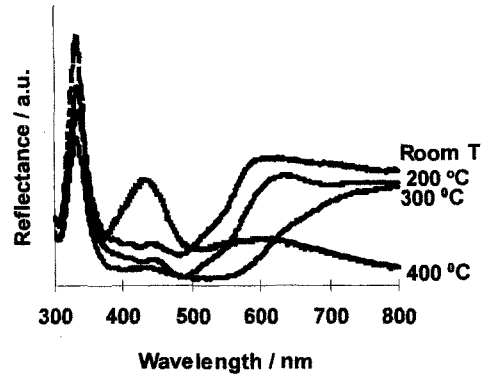

Figure 3. UV-vis reflectance spectra of the $Ru(bpy)_3^{2+}$ intercalated oxides heated at different temperatures.

The UV-vis reflectance spectra of the $Ru(bpy)_3^{2+}$ intercalated sample are given in Figure 3 before and after heat treatment at different temperatures. The absorption edge due to the MLCT of the $Ru(bpy)_3^{2+}$ at 590 nm at room temperature shifted to the red and the band broadened by heat-treatment. The shift was assigned to the strained complex molecules[3, 6] and to the chelate-oxide and chelate-chelate interaction[4]. The shift is also ascribable to the advancement in the interaction due to the removal of the surrounding water molecules by 200-300 °C. The original pyridine values in the finger print 1300-1700 cm^{-1} region for the sample heated at 300 °C was still observable in the FTIR spectrum, but not for the samples heated at 400 °C.

During the submersion of the film/substrate into the K_2SO_4 electrolyte the intercalated complex cations with the exception of the $Ag(NH_3)_2^+$ intercalated and the heat-treated $Ru(bpy)_3^{2+}$ intercalated samples dissolved from the interlayer into the solution. The $Ru(bpy)_3^{2+}$ intercalated films at room temperature experienced the contraction of the layer distance from 16.6 Å to 9.3 Å because of the deintercalation of the $Ru(bpy)_3^{2+}$ into the K_2SO_4 solution by ion exchange between the $Ru(bpy)_3^{2+}$ and K^+ due to the XPS analysis. The easy exchange is due to the weak interaction between the intercalated complexes and the host Ti-O layers. The $Ru(bpy)_3^{2+}$ intercalated sample heat-treated at 300 °C, however, kept its single-phase layered structure without any change, even after continuous potential sweep over 2 hours. This is based on the strong interaction between the pyridine in the $Ru(bpy)_3^{2+}$ and the Ti-O host layer.

The $Ru(bpy)_3^{2+}$ and $Ag(NH_3)_2^+$ intercalated samples went through the redox reactions of the intercalated complexes. The degree of the interaction of the complex with the Ti-O host layer determines whether the system undergoes a redox reaction. A charge transfer bridge occurs through the strongly interacted Ru^{2+}-ligand and weakly interacted ligand-host layer couples for $Ru(bpy)_3^{2+}$ intercalated sample. In the case of $Ag(NH_3)_2^+$ intercalated sample, center Ag^+ directly interacts with the Ti-O host layer. Thus, the electron transfer through the Ti-O host layers via the interactions like a resonance tunneling results in the redox reactions of the intercalated complex cations. For the hexaammine complex $[M(NH_3)_6^{n+}]$ intercalated samples, however, ligand-host layer and metal – ligand interactions are too weak to transfer the electron and the NH_3 ligands surrounding the center M^{n+} suppress the direct interaction of the M^{n+} with the Ti-O host layer.

The cyclic voltammogram of the non-heated $Ru(bpy)_3^{2+}$ intercalated sample exhibited redox reaction in the region from 1 to 1.2 V due to the Ru(II)/Ru(III) for $Ru(bpy)_3^{2+}$ complex. After the oxidation of Ru(II) to Ru(III), the system produced photocurrent due to the hole produced in the Ti-O host layers under UV illumination. Only very low photocurrent was observed in the Ru(II) region, because Ru(II) acts as the recombination center between the excited electron and hole in the Ti-O host layer, but not Ru(III). During the redox reaction, an intercalation/release of the solution cations (K^+ and/or H_3O^+) should take place simultaneously, because the system has to keep the neutrality of the layered oxide during the electrochemical reaction.

On the other hand, the heat-treated sample at 300 °C exhibited no deintercalation and no redox reaction. However, the heated sample exhibited both anodic and cathodic photocurrents even under visible light illumination, as seen in Figure 4, where the light with a wavelength shorter than 420 nm was cut by a cut-off filter. The $Ru(bpy)_3^{2+}$ molecule in the layer absorbs the visible light and is excited to MLCT state to form $Ru(bpy)_3^{2+*}$, which leads to the photocurrent. The changing potential from the cathodic to anodic photocurrent is in the range from 0.3 to 0.6 V (two arrows in the figure), which corresponds to the flat band potential. Electrons produced by the excitation from the HOMO level to the LUMO level of the $Ru(bpy)_3^{2+}$ under irradiation will go into the conduction level (CB) of the Ti-O host layers, and will move through the CB levels. On the other hand, the produced hole will also move by the tunneling mechanism, where the hole or electron moves through the LUMO levels. The cathodic and anodic photoelectrochemical reactions will result in the H_2 and O_2 evolution, respectively, according to the energy positions.

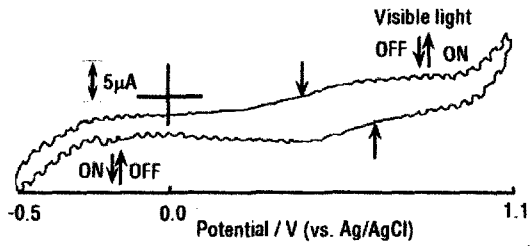

Figure 4. Cyclic Voltammograms of the $Ru(bpy)_3^{2+}$ intercalated oxide heat-treated at 300 °C. The arrows in denote the changing potentials from anodic to cathodic photocurrents.

The cyclic voltammogram of the $Ag(NH_3)_2^+$ intercalated sample in the dark is given in Figure 5. The system underwent an irreversible reduction of the interlayer silver molecules to Ag metal in the first cycle and then possessed only reversible Ag/Ag_2O redox reaction in the following cycles according to the equilibrium potentials. The illumination resulted in the production of the small photocurrent in the first cathodic sweep. The color of the electrode has changed from white to silver after the first cycle under illumination as a result of the formation of the coarse Ag metal particulates by the illumination of UV light. In the case of the second cycle under illumination, the photocurrent disappeared. Thus, low-enough aggregation level of the silver metal atoms at the first cycle is the reason of the photoresponse. In other words, the photoresponse is due to the formation of the atomic and/or nano-level Ag metal in the interlayer, while the coarse Ag metal particulates formed in the interlayer bring about no photoresponse. The formation of the Ag metal clusters by aggregation of the atomic and/or nano-level Ag is photo-assisted in the interlayer in the presence of the UV light and TiO_6 layers[6]. The dependency of the photocurrent on the amount of silver in different systems has been also reported in previous studies[9,10].

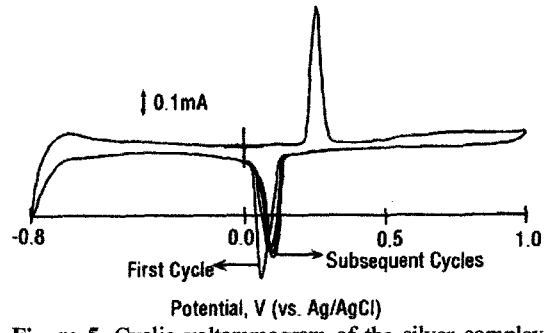

Figure 5. Cyclic voltammogram of the silver complex intercalated film under no illumination.

In conclusion, we have reported that the new technique (ESD) facilitates the easier and quick intercalation of molecules or cations into the interlayer of the layered oxides. In addition, the type of cations determines the stability of layered oxides. In electrochemical measurements, both $Ru(bpy)_3^{2+}$ and $Ag(NH_3)_2^+$ intercalated samples where some interactions between the complex cations and Ti-O layer are present, showed the redox reactions. For these samples, a tunneling mechanism through the Ti-O host layers was proposed. The $Ru(bpy)_3^{2+}$ intercalated film heated at 300 °C, where relatively strong interaction of the pyridine/Ti-O host layer is formed, showed the visible light photocurrent due to the excitation of the electrons from the HOMO to the LUMO levels.

We acknowledge the kindly help and support granted by the Core Research for Evolutional Science and Technology (CREST) group.

4. REFERENCES

[1] U. Unal, D. Matsuo, Y. Matsumoto and M. Koinuma, *J. Mater.Res.*, **17(10)**, 2644 (2002).
[2] T. Sasaki, F. Izumi, and M. Watanabe, *Chem. Mater.*, **8**, 777 (1996).
[3] T. Nakato, D. Sakamoto, K. Kuroda, and C. Kato *Bull. Chem. Soc. Jpn.*, **65**, 322 (1992).
[4] K. Yao, S. Nishimura, Y. Imai, H. Wang, T. Ma, E. Abe, H. Tateyama, and A. Yamagishi, *Langmuir*, **19**, 321 (2003)
[5] T. Sasaki, M. Watanabe, Y. Komatsu and Y. Fujiki, *Inorg. Chem.*, **24**, 2265 (1985).
[6] T. Sumida, Y. Takahara, R. Abe, M. Hara, J.N. Kondo, K. Domen, M. Kakihana, and M. Yoshimura, *Phys. Chem. Chem. Phys.*, **3**, 640 (2001).
[7] J.H. Choy, H.C. Lee, H. Jung, H. Kim, and H. Boo, *Chem. Mater.*, **14**, 2486 (2002).
[8] Y. Matsumoto, A. Funatsu, D. Matsuo, U. Unal, and K.J. Ozawa, *J. Phys. Chem. B*, **105(44)**, 10893 (2001).
[9] V. Vamathevan, H. Tse, R. Amal, G. Low and S. McEvoy, *Catalysis Today*, **68**, 201 (2001).
[10] C. Wen, K. Ishikawa, M. Kishima, and K. Yamada, *Solar Energy Materials & Solar Cells*, **61**, 339 (2000).

(Received October 11, 2003; Accepted March 13, 2004)